High temperature H$_2$/CO$_2$ separation using cobalt oxide silica membranes

S. Smart [a]
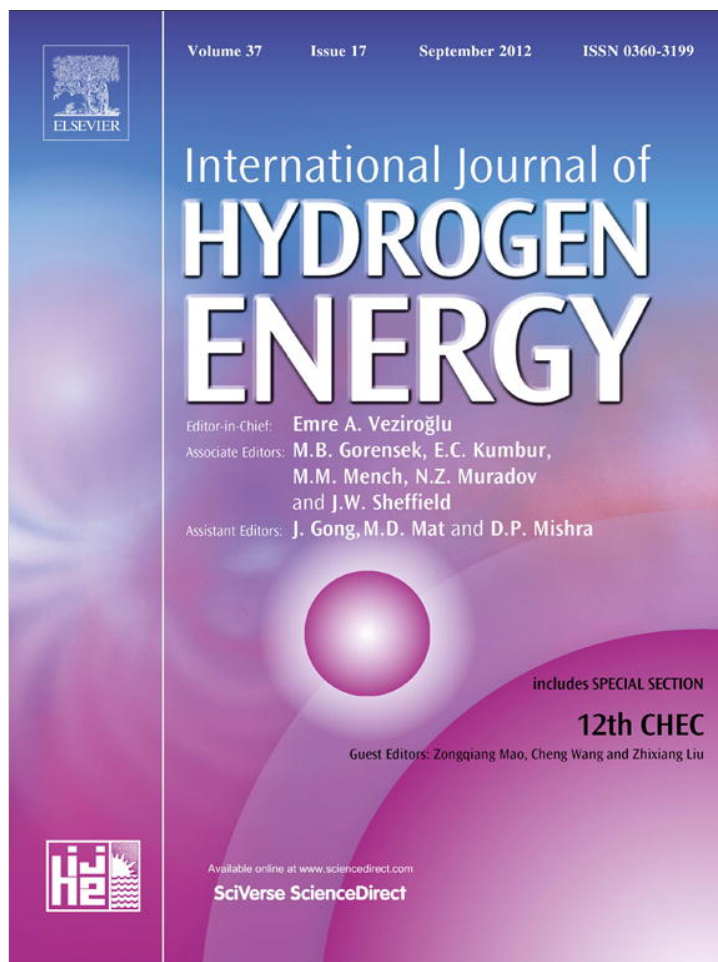
J.F. Vente [b]

J.C. Diniz da Costa [a]

[a] *The University of Queensland, FIMLab - Films and Inorganic Membrane Laboratory, School of Chemical Engineering, Brisbane, Qld 4072, Australia*

[b] *Energy Research Centre of the Netherlands, P.O. Box 1, 1755 ZG Petten, The Netherlands*

Available online at www.sciencedirect.com

SciVerse ScienceDirect

journal homepage: www.elsevier.com/locate/he
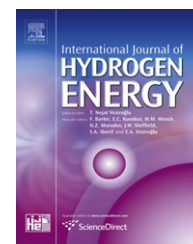
High temperature H_2/CO_2 separation using cobalt oxide silica membranes

S. Smart [a], J.F. Vente [b], J.C. Diniz da Costa [a],*

[a] The University of Queensland, FIMLab — Films and Inorganic Membrane Laboratory, School of Chemical Engineering, Brisbane, Qld 4072, Australia
[b] Energy Research Centre of the Netherlands, P.O. Box 1, 1755 ZG Petten, The Netherlands

ARTICLE INFO

ABSTRACT

In this work high quality cobalt oxide silica membranes were synthesized on alumina supports using a sol–gel, dip coating method. The membranes were subsequently connected into a steel module using a graphite based proprietary sealing method. The sealed membranes were tested for single gas permeance of He, H_2, N_2 and CO_2 at temperatures up to 600 °C and feed pressures up to 600 kPa. Pressure tests confirmed that the sealing system was effective as no gas leaks were observed during testing. A H_2 permeance of 1.9×10^{-7} mol m^{-2} s^{-1} Pa^{-1} was measured in conjunction with a H_2/CO_2 permselectivity of more than 1500, suggesting that the membranes had a very narrow pore size distribution and an average pore diameter of approximately 3 Å. The high temperature testing demonstrated that the incorporation of cobalt oxide into the silica matrix produced a structure with a higher thermal stability, able to resist thermally induced densification up to at least 600 °C. Furthermore, the membranes were tested for H_2/CO_2 binary feed mixtures between 400 and 600 °C. At these conditions, the reverse of the water gas shift reaction occurred, inadvertently generating CO and water which increased as a function of CO_2 feed concentration. The purity of H_2 in the permeate stream significantly decreased for CO_2 feed concentrations in excess of 50 vol%. However, the gas mixtures (H_2, CO_2, CO and water) had a more profound effect on the H_2 permeate flow rates which significantly decreased, almost exponentially as the CO_2 feed concentration increased.

1. Introduction

The dominant role of hydrogen in a sustainable energy future is widely accepted [1], though cost effective approaches to separate hydrogen from gas mixtures are required. Hydrogen can be generated from water splitting [2–5], fossil fuels [6,7] and biomass [8–10]. Conventionally hydrogen is industrially produced via high temperature processes such as natural gas reforming. High temperature gas separation is therefore desirable in many industrial processes in order to reduce efficiency losses associated with cooling down gas streams [11]. To address this industrial requirement, inorganic membranes have been developed for high temperature operation, particularly those having molecular sieving properties to take advantage of their activated transport properties. Examples include pure silica [12–14], templated silica [15–17], hybrid organosilica [18–20] and metal or metal oxide doped silica [21–23] membranes. A key feature of these silica derived

membranes is the flux of gases with kinetic diameters below ∼3 Å such as He ($d_k = 2.6$ Å) and H_2 ($d_k = 2.89$ Å) increases with temperature, and generally complies with the phenomenological activated transport equation (Equation (1)) [24], which was derived from Barrer's model [25]:

$$J \propto J_0 \exp\left(\frac{-E_{act}}{RT}\right) \tag{1}$$

where J is the flux (mol m^{-2} s^{-1}) through the membrane, E_{act} (kJ mol^{-1}) is an apparent activation energy, R the gas constant and T the absolute temperature (K). Conversely, the flux of gases with kinetic diameters above ∼3 Å such as CO_2 ($d_k = 3.3$ Å) and N_2 ($d_k = 3.64$ Å), having a negative activation energy, decreases with temperature. Therefore, in addition to an increase in flux for smaller gases like H_2 there should also be a corresponding increase in separation from larger gases like CO_2 with temperature. These attributes have made molecular sieve silica (MSS) membranes the focus of significant research into gas separation at high temperature process conditions.

Despite this potential, reports of testing MSS membranes in industrially relevant gas mixtures or at high temperatures are very limited in the literature (Table 1). Indeed, the vast majority of literature has focussed on single gas permeation data as a means of establishing membrane performance parameters. Whilst single gas permeation is certainly a rapid and universally comparable testing regime, it is not particularly relevant to industrial applications. Those studies willing to undertake the more complex testing have reported significant differences in both membrane separation ability and flux for gas mixtures as compared to single gases [26]. Thus there is a need for more studies that investigate MSS membranes for separation of gas mixtures. With regards to the lack of high temperature testing, there are several reasons for this limitation. Firstly, efficient sealing technology using polymeric o'rings is generally limited to 200 °C, although some (such as Kalrez o'rings) can operate up to 315 °C. Above these temperatures, graphite-based seals and gaskets can provide a good solution, but as membrane development moves from platelets to tubular supports another technical problem is

encountered – ceramic tubes tend to crack and shear at the seal and ceramic tube interface [11,27]. The second problem is that the matrix of MSS membranes tends to densify for temperatures in excess of 500 °C, as condensation reactions eliminate remaining silanol groups to form dense siloxane networks [28]. As a result of this densification, membrane flux and separation performance decreases significantly.

The majority of high temperature testing of MSS membranes published thus far has generally been in chemical vapour deposition (CVD) silica membranes [29–32], and specifically for single gas permeation. Indeed sol–gel silica membranes have not been tested in excess of 500 °C and even then only in very few cases (Table 1). CVD membranes are a special case, as these membranes are generally prepared with a very small surface area in the central region of a ceramic tube, while the remaining tube surface has a dense ceramic layer [33]. This design allows for the membrane seals to be placed outside the high temperatures of the heating zone, reducing any significant heat stress on the seals. The difficulty of this design in terms of engineering applications is that a significant portion of surface area of the tubular support is lost in order to keep the seals outside the heating zone. Hence membranes manufactured in this manner will require large unit operations with small surface area packing density, which translates into large capital costs. Further, CVD membranes are traditionally made in situ before testing [34], which is also not feasible for industrial applications. Nevertheless, CVD silica membranes have demonstrated excellent capabilities as outlined in Table 1.

Efforts to improve microporous silica membrane materials has recently seen the embedding of metal oxides into silica films which has been shown to be beneficial in terms of hydrostability and thermal stability of silica derived membranes, particularly focusing on H_2 separation. Various metal oxides have been trialled and cobalt and nickel oxides have been shown to give the best performance for H_2 separation in conventional membrane units [22,23,37], or in a membrane reactor arrangement [38–41]. Recently, Yacou and co-workers [26] reported that MSS membranes doped with cobalt oxide were thermally stable for dry gas separation up to

Table 1 – List of membrane testing conditions above 300 °C.

Membrane	H$_2$ permeation (mol m^{-2} s^{-1} Pa^{-1})	Permselectivity	Temperature (°C) pressure (kPa)	Sealing system
MTES-templated Silica [12]	1.9×10^{-6}	6 (H_2/CO_2)	300 °C 350 kPa	Not given/Plate type membrane
Silica Zirconia [35]	2.0×10^{-9}	37 (H_2/CO_2)	300 °C	Not given/tubular membrane
Nickel-Silica [36]	1.1×10^{-6} (He)	260 (He/N_2)	300 °C 200 kPa	Not given/tubular membrane
Nickel-Silica [37]	4.5×10^{-7}	370 (H_2/N_2)	500 °C 500 kPa	Not given/tubular membrane
Surfactant templated silica [17]	4.2×10^{-6}	35 (H_2/CO_2)	400 °C 260 kPa	Not given/tubular membrane
Cobalt-Silica [21]	1.8×10^{-7}	730 (H_2/N_2)	500 °C 500 kPa	Not given/tubular membrane
Silica-CVD [33]	1.1×10^{-7}	1000 (H_2/CO_2)	600 °C 160 kPa	Glazed to dense alumina tubing/sealing outside heating zone
Silica-Alumina-CVD [34]	1.6×10^{-7}	590 (H_2/CO_2)	600 °C 200 kPa	Glazed to dense alumina tubing/sealing outside heating zone

500 °C for 2000 h operation. The nanoparticles of nickel or cobalt in the silica matrix may confer the ability to reduce the thermally induced molecular motion of the silica membrane network during thermal and hydrothermal degradation [21]. It has also been shown that the inclusion of cobalt as a dopant reduces water adsorption, offering increased resistance by decreasing the hydrophilicity of silica [42].

In this work, we test a more integrated approach to producing inorganic membrane systems for high temperature gas separation. In our design, the membrane tube is fully coated with a cobalt oxide silica film, and the entire membrane length including seals is tested within a single heating zone. This is particularly significant as both membrane and seals are exposed to the same temperatures, allowing the development of a high packing density, high surface area and low volume unit operation. We further investigate the robustness of cobalt silica membranes to cope with temperatures higher than 500 °C, the point where conventional MSS membranes start to densify, by choosing operating conditions up to 600 °C and 600 kPa feed pressure for both single gas permeation of He, H_2, CO_2 and N_2, and more importantly for a series of industrially relevant H_2/CO_2 binary mixtures. The seals used are also tested for their ability to operate leak free under all manner of gas testing conditions.

2.   Experimental

Cobalt silica sol—gel solutions were synthesised from tetrathylorthosilane (TEOS), ethanol (EtOH), 30% hydrogen peroxide (H_2O_2) in water (H_2O) and cobalt nitrate hexahydrate ($Co(NO_3)_2.6H_2O$) as described elsewhere [23], with a final molar ratio of 255 EtOH:4 TEOS:1 $Co(NO_3)_2.6H_2O$: $9H_2O_2$: $40H_2O$. Xerogel samples were prepared from sol-gels dried in an oven at 60 °C under controlled humidity conditions. Xerogel samples were subsequently crushed and calcined at different temperatures ranging from 500 to 800 °C. The calcination process involved a ramp rate of 2 °C min^{-1} until a desired temperature was achieved with a dwell time of 2 h, following by cooling similar to the ramp rate. Calcined xerogel samples were then degassed overnight at 200 °C and tested for pore N_2 adsorption using a Micromeritics Tristar 3000.

Cobalt oxide silica thin film layers were coated on ceramic tubular supports 10 cm in length and 1.4 cm external diameter. The manufacturing of these γ-alumina supports provided by the Energy Centre of the Netherlands are described elsewhere [43]. These supports have an intrinsic pore size distribution centered ~4 nm, with a very low defect

density above 10 nm. The tubular supports were dip-coated with the cobalt silica sol using a controlled immersion time of 1 min, and immersion/withdrawal speed of 10 cm min^{-1}. Each layer was calcined at 630 °C in air, and held for 2.5 h with a heating and cooling rate of 1 °C min^{-1}. A total of 4 layers of cobalt silica sol gel solution were coated onto the alumina support.

Subsequently, the membrane tube was sealed as shown in Fig. 1. This seal involves a patented graphite seal at the interface between the membrane and a stainless steel cap [44]. This sealing technology requires longitudinal compressive force and avoids the common problem tube cracking caused by excessive compressive radial or shearing force between the seal and ceramic tube. The sealing cap is then welded to an appropriate stainless steel fitting for testing.

Single gas permeation tests were conducted up to 600 °C and feed pressures of 600 kPa (limited by Occupational Health and Safety laboratory regulations). The membrane module was housed in a furnace where the temperature was controlled via a thermocouple inserted in the inner shell of the membrane tube connected to an external PID temperature controller to the furnace. The pressure of the gas feed stream was measure by MKS pressure transducers. The single gas permeation tests were carried out at dead end mode for the retentate stream, while the permeate stream was open to the atmosphere. The gas flow rates in the permeate stream were measured by a bubble flow meter. The permeance of gas species i, P_i (mol s^{-1} m^{-2} Pa^{-1}) was calculated as per Equation (2):

$$P_i = \frac{J_i}{\Delta p} \qquad (2)$$

where J_i is the molar flux (mol s^{-1} m^{-2}) of gas species i and Δp is the transmembrane pressure difference (Pa). Permselectivity of species i to species j, $S_{i/j}$ was calculated as the ratio of permeances of the respective gases measured at the same temperature and pressure, as shown in Equation (3):

$$S_{i/j} = \frac{P_i}{P_j} \qquad (3)$$

Binary mixtures of H_2 and CO_2 were mixed in a custom gas mixing rig controlled through MKS mass flow controllers. The feed pressure was kept at 500 kPa via a backpressure regulator on the retentate outlet. Total permeate gas concentrations were determined by gas chromatograph Shimadzu GC-2014 with TCD and FID detectors. The flow rate (l s^{-1}) of H_2 was calculated by multiplying the H_2 concentration by the permeate flow rate measured by a bubble meter. The operation conditions for the binary gas mixture separation are listed in Table 2.

Fig. 1 — **Cobalt oxide silica membrane sealed with ECN proprietary graphite sealing technology [44].**

Table 2 — Operating conditions for mixed gas testing at 500 kPag.			
Feed gas composition	Temperature (°C)	Feed flow rate (l h^{-1})	Stage cut
90% H$_2$/10% CO$_2$	600	7.3	0.5
	500	5.6	0.34
	400	4.5	0.23
80% H$_2$/20% CO$_2$	600	5.3	0.58
	500	1.9	0.28
70% H$_2$/30% CO$_2$	400	2	0.21
50% H$_2$/50% CO$_2$	600	0.4	0.75
55% H$_2$/45% CO$_2$	500	1.4	0.16
	400	1	0.16
20% H$_2$/80% CO$_2$	600	0.1	0.25
10% H$_2$/90% CO$_2$	500	0.2	0.03
20% H$_2$/80% CO$_2$	400	0.3	0.01

Fig. 3 — N$_2$ Isotherms for cobalt oxide silica samples calcined at temperatures from 500 °C to 800 °C — adsorption (line) and desorption (symbol).

3. Results and discussion

Fig. 2 shows an SEM micrograph of the cross section of the membrane used in this work. The membrane was comprised of a base support of large coarse α-alumina particles, followed by 2 interlayers of ∼30 μm depth each of smaller α-alumina particles and by 2 γ-alumina layers of total ∼3 μm depth. The smooth interlayer structure allowed for the coating of the cobalt oxide silica top film with an average thickness of ∼60 nm. This asymmetric substrate and layering fabrication system gives the highest resistance to gas diffusion at the top cobalt oxide silica layer, which is sequentially reduced through the interlayers until the lowest flux resistance of the substrate.

The nitrogen isotherms of cobalt silica xerogels samples calcined between 500 and 800 °C are shown in Fig. 3. These isotherms are of Type I, characteristic of highly microporous materials. It is observed that the total pore volume reduces with the calcination temperature, which in turn also reduces the BET surface area as displayed in Fig. 4. Conventional
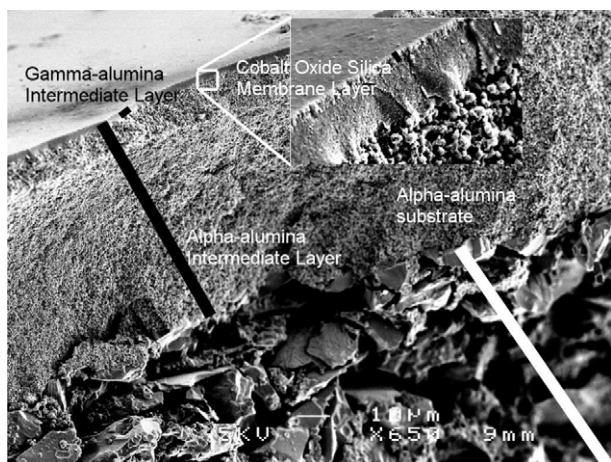
microporous silica xerogels tend to experience significant densification above 500 °C [28], resulting in dense, non-porous structures. However, in the case of the cobalt silica xerogel, significant densification is not observed until 800 °C, indicating the cobalt oxide nanoparticles embedded in the silica matrix appear to provide superior structural stabilization to the silica matrix and prevent significant densification. Of significant interest, a maximum surface area and pore volume is observed at 600 °C. This is counter intuitive as the surface

Fig. 2 — Cross-section of cobalt silica membrane as observed via SEM (5 keV). The black and white bars are guides to identify the substrate, the various interlayers and the membrane layer itself (insert).
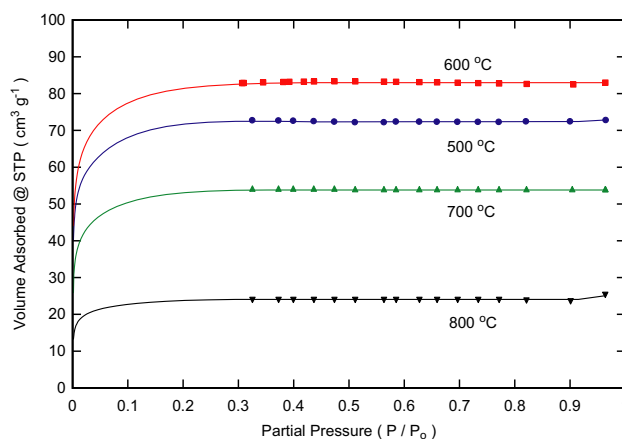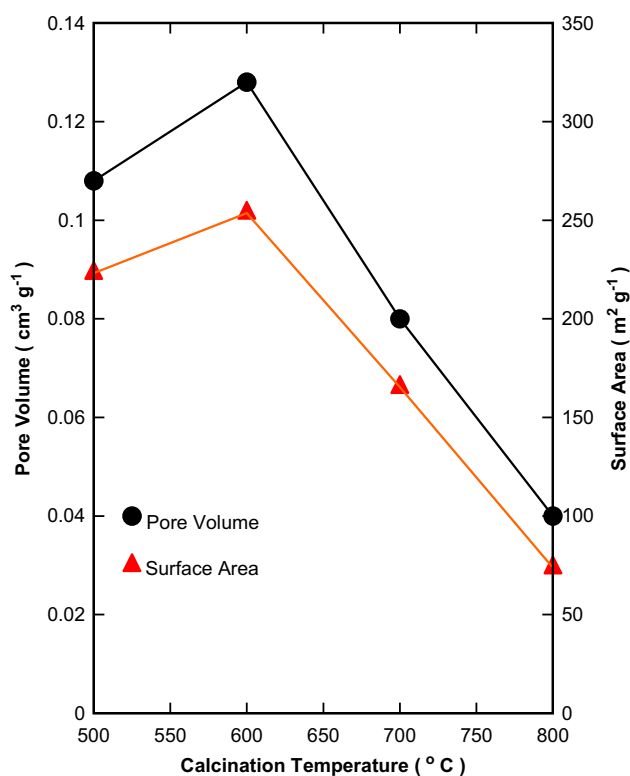

Fig. 4 — BET surface area and pore volumes of cobalt oxide silica xerogel samples calcined at temperatures from 500 °C to 800 °C.

area and pore volume of silica derived xerogels should reduce with the increased calcination temperature, particularly above 500 °C. The embedding of cobalt oxide nanoparticles into the silica matrix clearly demonstrates that the cobalt oxide nanoparticles opposed the collapse of the silica matrix. Therefore, the cobalt oxide nanoparticle added a beneficial thermal resistance to silica structure [21]. Although the surface area and pore volume reduced at 600 °C, it is remarkable to observe that the hybrid xerogels were still able to resist densification at high temperatures, which traditionally deliver non-porous silica structures.This key finding motivated us to test our cobalt silica membranes up to 600 °C, which is at least 100 °C higher than any previously published study using MSS-based membranes prepared via sol−gel techniques.

Fig. 5 shows the H_2 permeance through the membrane as a function of the cross-membrane pressure difference at temperatures ranging from 200 °C−600 °C. The results clearly show that membrane permeance does not significantly depend on the feed pressure. The small variations observed are more likely associated with small temperature changes, which affected gas permeation due to the molecular sieving nature of the cobalt oxide silica membrane. These results suggest that the contribution from viscous flow can be ignored, that the membrane is free of defects and that the sealing technology is leak free under the current testing conditions.

Fig. 6 shows the single gas permeance data for He, H_2, N_2 and CO_2 tested at 200 °C−600 °C with a cross-membrane pressure difference of 550 kPa. The permeance of N_2 and CO_2 was below the detection limit (flux ≤ 0.003 ml s^{-1}). In each case the permeance for the gases was calculated by normalising the lowest detectable molar flux against the tested pressure, which yielded a permeance $\leq 1.1 \times 10^{-10}$ mol m^{-2} s^{-1} Pa^{-1}. In contrast, the permeance of He and H_2 increased by one order of magnitude, as the temperature rose from 200 °C−600 °C. The He/N_2 and H_2/CO_2 permselectivities (using the permeance values for N_2 and CO_2 calculated as previously described) ranged from 380 to 250 at 100 °C to 1740 and 1530 at 600 °C respectively, which, taken in
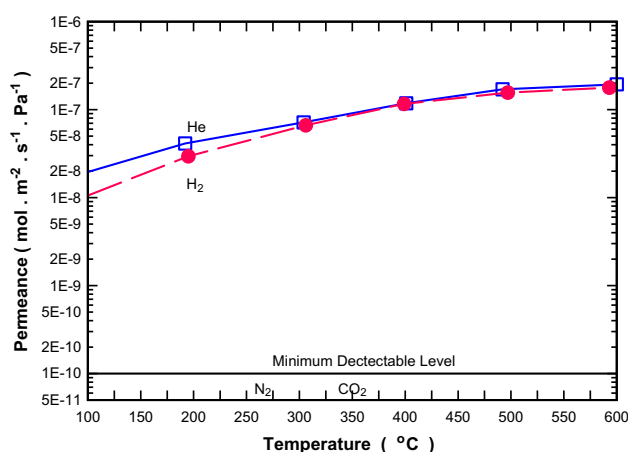
Fig. 6 − Single gas permeance (±8%) at temperatures ranging from 200 °C to 600 °C for a transmembrane pressure of ΔP = 500 kPa.

conjunction with the high H_2 permeation shows the preparation of high quality MSS tube geometry membrane derived from sol−gel methods. The apparent activation energy for the permeance of the various gases was calculated based on an Arrhenius relation of the natural log of permeance over the inverse of temperature and was found to 13.2 and 15.6 kJ mol^{-1}, for He and H_2 respectively. Interestingly, both the permeance values and the apparent activation energies are greater for H_2 than for He indicating that the transport of H_2 through the membrane is not solely a molecular sieving mechanism, but is boosted by the presence of cobalt oxide. This effect has been reported for other metal and metal oxide silica membranes [22,26,45,46] and the apparent activation energies are also in the range of those values reported elsewhere for H_2 (12.8−21.3 kJ mol^{-1}) [21,47] and He (9.5−20.7 kJ mol^{-1}) [23,47]. The apparent activation energy of N_2 and CO_2 could not be calculated as the permeance was below the detection limit for all temperature points tested.

These results demonstrate that the incorporation of cobalt oxides into the silica matrix not only produced a more thermally stable structure, able to overcome thermally induced densification, but also delivered a microstructure with very precise pore tailorability. This is evidenced by the high permeation results of He and H_2, coupled with the high permselectivity of the membrane for the smaller gases. These results clearly demonstrate the effectiveness of the sealing design and the quality of the sol−gel derived cobalt silica membranes. The selection of the steel 316L in the design of the membrane module limited any tests in excess of 600 °C at the feed pressures desired. In other words, the testing was no longer limited by either the supports, the selective membrane layers or the seals, but the steel of the membrane module itself.

The membranes were further tested for binary gas mixtures of H_2 and CO_2 at high temperatures, starting at 600 °C and followed by 500 °C and finally down to 400 °C as shown in Fig. 7. At each temperature set, the binary mixture was initially set at high H_2 concentrations, and subsequently reduced, finishing with high CO_2 concentrations. The first
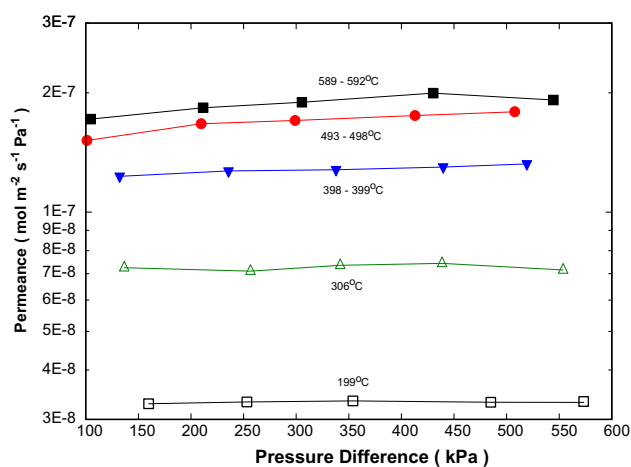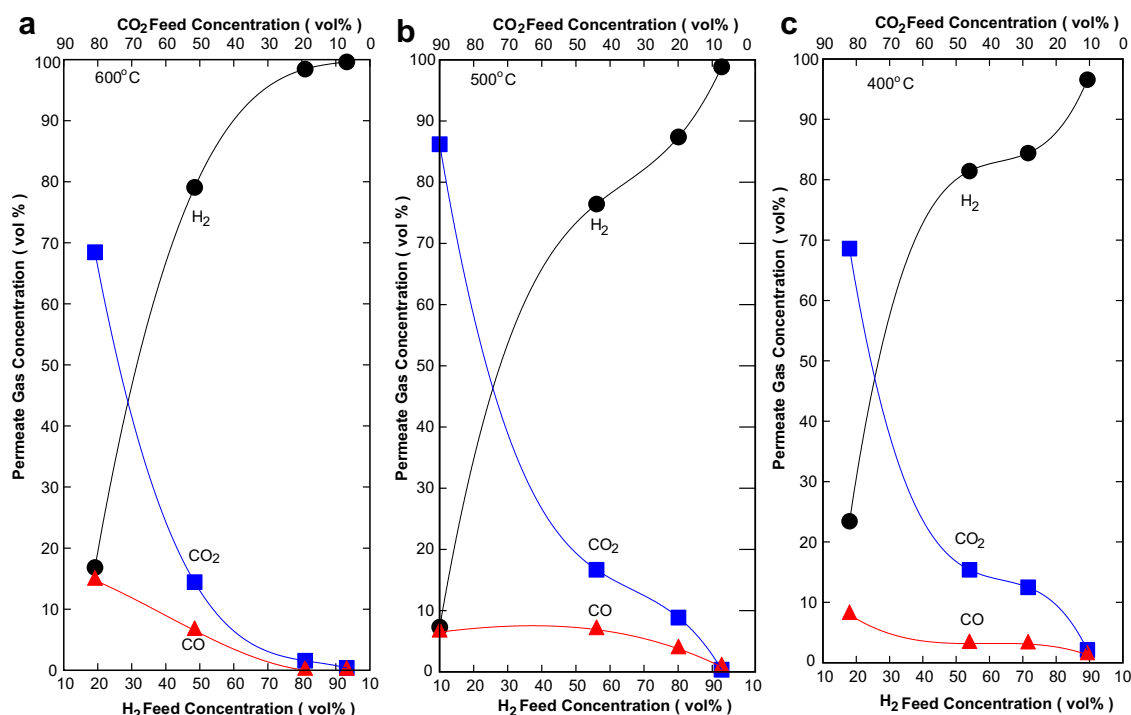

Fig. 5 − Single gas H_2 permeance (±8%) as a function of cross-membrane pressure (±5%) at operating temperatures from 200 °C to 600 °C.

Fig. 7 – Permeate gas concentration (±10%) from a cobalt oxide silica membrane as a function of the H_2/CO_2 binary feed concentration at (a) 600 °C, (b) 500 °C and (c) 400 °C.

important observation is that at these high temperatures and in tandem with the catalytic action of both the cobalt oxide in the silica matrix and the metals in the steel 316L membrane module, these conditions allowed for the reverse of the water gas shift reaction to occur ($CO_2 + H_2 \rightarrow CO + H_2O$). CO started forming, and water was observed (condensed in the permeate and retentate streams), for H_2/CO_2 feed molar ratios of 50/50 at 600 °C. From there on CO measurement and water condensation was detected at all temperatures and binary gas mixture compositions. In addition, the concentration of CO increased as a function of the feed CO_2 concentration. The membrane generally performed well for H_2/CO_2 feed concentrations up to 50/50 binary feed mixtures, as exemplified by H_2 permeate concentration ∼80% at 600 °C. As the concentration of H_2 increased in the feed stream, so did it in the permeate stream. It is noteworthy that very high H_2 permeate concentrations in excess of 98% were measured at 600 °C for a binary feed mixture of 80/20, though the membrane delivered lower values, above 85%, at 500 and 400 °C.

At these high temperature testing conditions, the membrane module actually behaved like a membrane reactor, and the intention of analysing the performance of the membrane for gas mixtures was more complex as CO and water were generated by the reverse of the WGS reaction. Despite excellent single gas permselectivities, for feed binary mixtures below 50/50, the membranes did not show any separation capability, furthermore it was observed that CO_2 preferentially permeated at very low H_2 feed concentrations, a direct result of the significant decrease in H_2 driving force for permeation. The results for the cobalt oxide silica membrane in this work follows similar trends reported for MSS membranes prepared by the sol–gel process

[48] and chemical vapour deposition [49] tested at temperatures below 300 °C. It is noteworthy that the membrane was still able to produce a permeate purity of greater than 80% using a feed binary mixtures of 50/50 even with the water from the reverse WGS present. For the rest of this analysis we will consider feed binary mixtures at or above 50/50.

At 600 °C and feed binary mixtures of 90/10 and 80/20, no CO and water were observed. Hence, the gas mixture had no reactions and in principle was a binary gas mixture only. The separation of gas mixtures are greatly affected by the concentration of the components in the gas mixture and process conditions [26,47]. Although the chemical potential of molecules in a gas mixture will ensure that the gases are homogeneously mixed, in fact CO_2 (17.6 kJ mol^{-1}) has higher isosteric heat of adsorption for than H_2 (6.0 kJ mol^{-1}) based on silicalites [50] which are generally close to values obtained for microporous silica materials. Hence, CO_2 is likely to preferentially adsorb on silica and hinder the passage of H_2, though at much lower surface coverage for the high temperatures used in this work. Nevertheless, silica has a non-isotropic structure, possibly having a ternary pore size distribution [51], though Uhlmann and co-workers [52] reported that the pore size of silica structure around cobalt oxide is possibly smaller than for the pure silica. Therefore, CO_2 can diffuse through cobalt oxide silica matrix and access the percolation pathways where pore sizes are larger than its kinetic diameter of 3.4 Å.

For binary mixtures containing CO_2 in excess of 50 vol%, the measured fluxes were very low and close to the minimum measurable values. In view of the inverse of the WGS reaction, the driving force for H_2 permeation was also

very low. For instance at 600 °C for a H_2/CO_2 binary feed mixture of 48/52 operating at a total pressure of 500 kPa the H_2 partial pressure difference is ∼12 (±2) kPa, which is too low to initiate permeation of H_2 through the membrane. An added factor of consideration here is that the concentration of CO significantly increased, indicating that similar amount of water was also present in the membrane module. Uhlmann and co-workers [53] reported that water permeation in cobalt oxide silica membranes increased as a function of temperature. Water has a kinetic diameter of 2.65 Å which is slightly smaller than H_2 of 2.65 Å [54]. As water adsorbs on cobalt oxide silica at high temperatures [53], though at a very low adsorption capacity, it is likely that water was competing to access the same percolation pathways accessible to H_2 only for dry gas separation. In the case of wet gas separation, the preferential diffusion of water has reduced the measured H_2 flow rates. In addition some degradation of the membrane performance is observed due to hydrothermal instability of the silica matrix, which is consistent with previously reported results for cobalt oxide silica membranes [53]. This degradation manifests as an irreversible decrease in both membrane flux and separation ability at similar feed molar ratios. For example at 80/20 and 90/10 feed H_2/CO_2 molar ratios, the permeate purity and flux is decreased at 500 and 400 °C, although it is impossible to accurately determine how much is due to water blocking access to the pores and how much is due to hydrothermal degradation. It is important to note however, that the membrane performance was not significantly altered by hydrothermal degradation which provides further evidence of the reinforcing effect of the cobalt oxide addition.

4.   Conclusions

Cobalt oxide silica xerogels opposed thermally induced densification of the silica matrix, thus forming microporous structures well in excess of 500 °C, the temperature at which severe densification traditionally becomes apparent in silica materials. The cobalt oxide silica tube membranes were assemble and sealed gas tight and tested for single gas permeance of He, H_2, N_2 and CO_2 up to 600 °C, with a feed pressure of 600 kPa. A H_2 permeation of 1.9×10^{-7} mol m^{-2} s^{-1} Pa^{-1} was observed in conjunction with a H_2/CO_2 permselectivity of more than 1500. Temperature and pressure tests confirmed the efficiency of the sealing system up to 600 °C. In addition, the membranes were tested for H_2/CO_2 binary feed mixtures between 400 and 600 °C. Due to the effect of metal components in the pressure vessel membrane module, the reverse of the water gas shift reaction occurred. As a result CO and water were generated, thus forming a quaternary gas mixture at the testing conditions. The concentration of CO increased as a function of CO_2 feed concentration. Consequently, the H_2 driving force decreased due to water formation thus reducing the purity of H_2 in the permeate stream, which was significantly affected for CO_2 feed concentrations in excess of 50 vol%. However, the gas mixtures had a more profound effect of H_2 permeate flow rates for the same reasons, which significantly decreased exponentially as the CO_2 feed concentration increased.

REFERENCES

[1] Muradov NZ, Veziroğlu TN. "Green" path from fossil-based to hydrogen economy: an overview of carbon-neutral technologies. Int J Hydrogen Energy 2008;33:6804—39.

[2] Dönitz W, Dietrich G, Erdle E, Streicher R. Electrochemical high temperature technology for hydrogen production or direct electricity generation. Int J Hydrogen Energy 1988;13: 283—7.

[3] Jing D, Guo L, Zhao L, Zhang X, Liu H, Li M, et al. Efficient solar hydrogen production by photocatalytic water splitting: from fundamental study to pilot demonstration. Int J Hydrogen Energy 2010;35:7087—97.

[4] Licht S. Thermochemical solar hydrogen generation. Chem Commun 2005:4635—46.

[5] Yan W, Zheng CL, Liu YL, Guo LJ. A novel dual-bed photocatalytic water splitting system for hydrogen production. Int J Hydrogen Energy 2011;36:7405—9.

[6] Bartels JR, Pate MB, Olson NK. An economic survey of hydrogen production from conventional and alternative energy sources. Int J Hydrogen Energy 2010;35:8371—84.

[7] Hotza D, Diniz da Costa JC. Fuel cells development and hydrogen production from renewable resources in Brazil. Int J Hydrogen Energy 2008;33:4915—35.

[8] Ferreira AF, Marques AC, Batista AP, Marques PASS, Gouveia L, Silva CM. Biological hydrogen production by Anabaena sp. − Yield, energy and CO2 analysis including fermentative biomass recovery. Int J Hydrogen Energy 2012; 37:179—90.

[9] Olivo C, Lebedeva I, Chu C-Y, Lin C-Y, Wu S-Y. A patent analysis on advanced biohydrogen technology development and commercialisation: scope and competitiveness. Int J Hydrogen Energy 2011;36:14103—10.

[10] Shimura K, Yoshida H. Heterogeneous photocatalytic hydrogen production from water and biomass derivatives. Energy Environ Sci 2011;4:2467—81.

[11] Smart S, Lin CXC, Ding L, Thambimuthu K, Diniz da Costa JC. Ceramic membranes for gas processing in coal gasification. Energy Environ Sci 2010;3:268—78.

[12] de Vos RM, Verweij H. Improved performance of silica membranes for gas separation. J Membr Sci 1998;143:37—51.

[13] Diniz da Costa JC, Lu GQ, Rudolph V, Lin YS. Novel molecular sieve silica (MSS) membranes: characterisation and permeation of single-step and two-step sol-gel membranes. J Membr Sci 2002;198:9—21.

[14] Tsai C-Y, Tam S-Y, Lu Y, Brinker CJ. Dual-layer asymmetric microporous silica membranes. J Membr Sci 2000;169: 255—68.

[15] de Vos RM, Maier WF, Verweij H. Hydrophobic silica membranes for gas separation. J Membr Sci 1999;158: 277—88.

[16] Duke MC, Diniz da Costa JC, Lu GQ, Petch M, Gray P. Carbonised template molecular sieve silica membranes in fuel processing systems: permeation, hydrostability and regeneration. J Membr Sci 2004;241:325—33.

[17] Pakizeh M, Omidkhah MR, Zarringhalam A. Synthesis and characterization of new silica membranes using template-sol-gel technology. Int J Hydrogen Energy 2007; 32:1825—36.

[18] Castricum HL, Paradis GG, Mittelmeijer-Hazeleger MC, Kreiter R, Vente JF, ten Elshof JE. Tailoring the separation behavior of hybrid organosilica membranes by adjusting the structure of the organic bridging group. Adv Funct Mater 2011;21:2319—29.

[19] Kanezashi M, Yada K, Yoshioka T, Tsuru T. Design of silica networks for development of highly permeable hydrogen separation membranes with hydrothermal stability. J Am Chem Soc 2008;131:414—5.

[20] Li G, Kanezashi M, Tsuru T. Preparation of organic—inorganic hybrid silica membranes using organoalkoxysilanes: the effect of pendant groups. J Membr Sci 2011;379:287—95.

[21] Igi R, Yoshioka T, Ikuhara YH, Iwamoto Y, Tsuru T. Characterization of co-doped silica for improved hydrothermal stability and application to hydrogen separation membranes at high temperatures. J Am Ceram Soc 2008;91:2975—81.

[22] Kanezashi M, Asaeda M. Hydrogen permeation characteristics and stability of Ni-doped silica membranes in steam at high temperature. J Membr Sci 2006;271:86—93.

[23] Uhlmann D, Liu S, Ladewig BP, Diniz da Costa JC. Cobalt-doped silica membranes for gas separation. J Membr Sci 2009;326:316—21.

[24] de Lange RSA, Keizer K, Burggraaf AJ. Analysis and theory of gas transport in microporous sol-gel derived ceramic membranes. J Membr Sci 1995;104:81—100.

[25] Barrer RM. Porous crystal membranes. J Chem Soc Faraday Trans 1990;86:1123—30.

[26] Yacou C, Smart S, Diniz da Costa JC. Long term performance cobalt oxide silica membrane module for high temperature H_2 separation. Energy Environ Sci 2012;5:5820—32.

[27] Duke M, Rudolph V, Lu GQ, Diniz da Costa JC. Scale-up of molecular sieve silica membranes for reformate purification. AIChE J 2004;50:2630—4.

[28] Brinker CJ, Scherer GW, Roth EP. Sol-Gel-Glass: II. Physical and structural evolution during constant heating rate experiments. J Non-Cryst Solids 1985;72:345—68.

[29] Araki S, Mohri N, Yoshimitsu Y, Miyake Y. Synthesis, characterization and gas permeation properties of a silica membrane prepared by high-pressure chemical vapor deposition. J Membr Sci 2007;290:138—45.

[30] Kim S, Gavalas GR. Preparation of H_2 permselective silica membranes by alternating reactant vapor deposition. Ind Eng Chem Res 1995;34:168—76.

[31] Nomura M, Ono K, Gopalakrishnan S, Sugawara T, Nakao S-I. Preparation of a stable silica membrane by a counter diffusion chemical vapor deposition method. J Membr Sci 2005;251:151—8.

[32] Rouessac V, Ferreira P, Durand J. Preparation of silica membranes inside macroporous alumina tubes by PECVD for hydrogen selectivity. Sep Purif Technol 2003;32:37—43.

[33] Lee D, Zhang L, Oyama ST, Niu S, Saraf RF. Synthesis, characterization, and gas permeation properties of a hydrogen permeable silica membrane supported on porous alumina. J Membr Sci 2004;231:117—26.

[34] Gu Y, Hacarlioglu P, Oyama ST. Hydrothermally stable silica-alumina composite membranes for hydrogen separation. J Membr Sci 2008;310:28—37.

[35] Yoshida K, Hirano Y, Fujii H, Tsuru T, Asaeda M. Hydrothermal stability and performance of silica-zirconia membranes for hydrogen separation in hydrothermal conditions. J Chem Eng Jpn 2001;34:523—30.

[36] Kanezashi M, Fujita T, Asaeda M. Nickel-doped silica membranes for separation of helium from organic gas mixtures. Sep Sci Technol 2005;40:225—38.

[37] Kanezashi M, Asaeda M. Stability of H_2-permeselective Ni-doped silica membranes in steam at high temperature. J Chem Eng Jpn 2005;38:908—12.

[38] Battersby S, Duke MC, Liu S, Rudolph V, Diniz da Costa JC. Metal doped silica membrane reactor: operational effects of reaction and permeation for the water gas shift reaction. J Membr Sci 2008;316:46—52.

[39] Oklany JS, Hou K, Hughes R. A simulative comparison of dense and microporous membrane reactors for the steam reforming of methane. Appl Catal A 1998;170:13—22.

[40] Tsuru T, Morita T, Shintani H, Yoshioka T, Asaeda M. Membrane reactor performance of steam reforming of methane using hydrogen-permselective catalytic SiO2 membranes. J Membr Sci 2008;316:53—62.

[41] Tsuru T, Yamaguchi K, Yoshioka T, Asaeda M. Methane steam reforming by microporous catalytic membrane reactors. AIChE J 2004;50:2794—805.

[42] Battersby S, Smart S, Ladewig B, Liu S, Duke MC, Rudolph V, et al. Hydrothermal stability of cobalt silica membranes in a water gas shift membrane reactor. Sep Purif Technol 2009; 66:299—305.

[43] Bonekamp BC, van Horssen A, Correia LA, Vente JF, Haije WG. Macroporous support coatings for molecular separation membranes having a minimum defect density. J Membr Sci 2006;278:349—56.

[44] Rusting FT, Pex PPAC, Peters JAJ. Sealing socket and method for arranging a sealing socket to a tube; 2003. US2003146625.

[45] Ikuhara YH, Mori H, Saito T, Iwamoto Y. High-temperature hydrogen adsorption properties of precursor-derived nickel nanoparticle-dispersed amorphous silica. J Am Ceram Soc 2007;90:546—52.

[46] Mori H, Fujisaki S, Saito T, Sumino T, Iwamoto Y. Characterisation of hydrogen interaction studies on cobalt doped amorphous silica composite materials for high temperature hydrogen separation membranes. 9th International Conference on inorganic membranes; 2006 [Lillehammer, Norway].

[47] Battersby S, Tasaki T, Smart S, Ladewig B, Liu S, Duke MC, et al. Performance of cobalt silica membranes in gas mixture separation. J Membr Sci 2009;329:91—8.

[48] Diniz da Costa JC, Lu GQ, Rudolph V. Permeation of binary gas mixtures in ultramicroporous membranes. J Nanosci Nanotechnol 2004;4:265—9.

[49] Gopalakrishnan S, Diniz da Costa JC. Hydrogen gas mixture separation by CVD silica membrane. J Membr Sci 2008;323: 144—7.

[50] Dunne J, Mariwala R, Rao M, Sircar S, Gorte RJ, Myers AL. Heats of adsorption of polar and non-polar gases in homogeneous and heterogeneous adsorbents. In: LeVan MD, editor. Fundamentals of adsorption. Boston (USA): Kluwer Academic Publishers; 1996. p. 227—84.

[51] Duke MC, Pas SJ, Hill AJ, Lin YS, Diniz da Costa JC. Exposing the molecular sieving architecture of amorphous silica using positron annihilation spectroscopy. Adv Funct Mater 2008;18: 3818—26.

[52] Uhlmann D, Smart S, Diniz da Costa JC. H_2S stability and separation performance of cobalt oxide silica membranes. J Membr Sci 2011;380:48—54.

[53] Uhlmann D, Smart S, Diniz da Costa JC. High temperature steam investigation of cobalt oxide silica membranes for gas separation. Sep Purif Technol 2010;76:171—8.

[54] Breck DW. Zeolite molecular sieves: structure, chemistry, and use. New York: Wiley; 1973.